Formation and Dissociation of Dimethyl Ether Clathrate Hydrate in Interstellar Ice Mimics

Bijesh K. Malla[1], Gaurav Vishwakarma[1], Soham Chowdhury[1], Samir Kumar Nayak[2], Sharma S. R. K. C. Yamijala[2,3,4,5] and Thalappil Pradeep[1,5,6]*

[1]Department of Science and Technology Unit of Nanoscience (DST UNS) and Thematic Unit of Excellence (TUE), Department of Chemistry, Indian Institute of Technology Madras, Chennai 600036, India.

[2]Department of Chemistry, Indian Institute of Technology Madras, Chennai, 600036 India,

[3]Centre for Atomistic Modelling and Materials Design, Indian Institute of Technology Madras, Chennai 600036, India.

[4]Centre for Quantum Information, Communication, and Computing, Indian Institute of Technology Madras, Chennai 600036, India.

[5]Centre for Molecular Materials and Functions, Indian Institute of Technology Madras, Chennai 600036, India,

[6]International Centre for Clean Water, IITM Research Park, Chennai 600113, India.

This PDF file includes:

Supporting information 1:

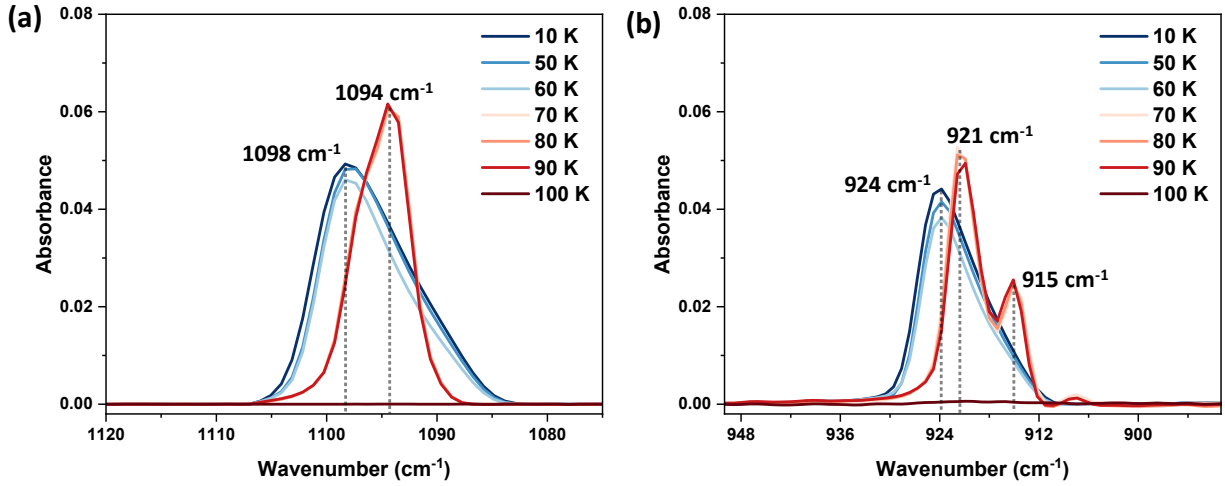

Figure S1. Temperature-dependent RAIR spectra of pure 150 ML DME in (a) C-O antisymmetric stretching region and (b) C-O symmetric stretching region. Pure DME vapor was deposited on Ru(0001) substrate at 10 K and annealed to 100 K with an annealing rate of 2 K min^{-1}. Vapor-deposited DME resulted in amorphous form at 10 K and crystallized above 70 K.

Supporting information 2:

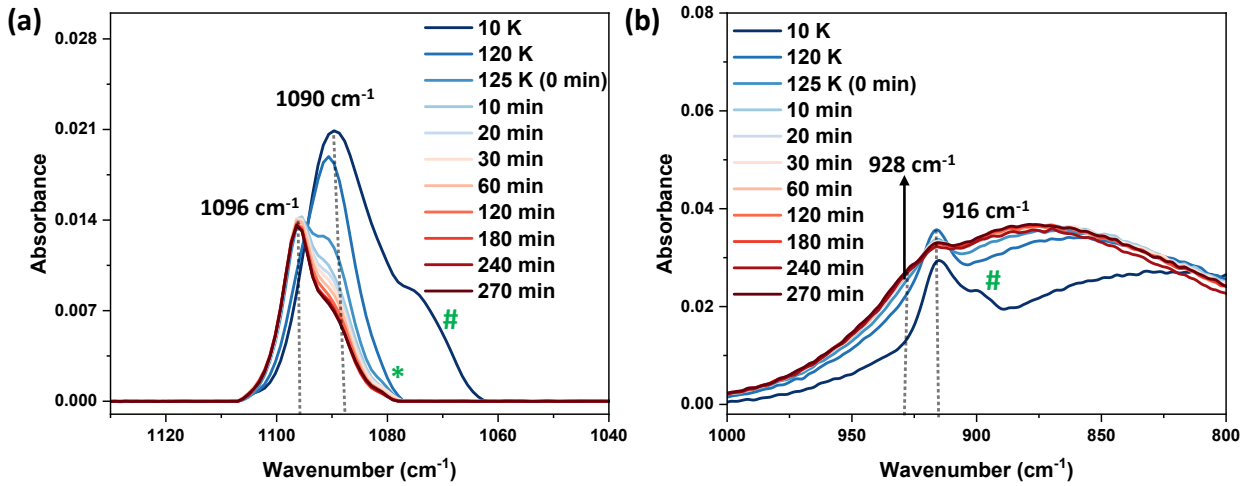

Figure S2. Temperature and time-dependent RAIR spectra of 300 ML of DME-H_2O (1:5) ice mixture in (a) C-O antisymmetric stretching region and (b) C-O symmetric stretching region. DME and water vapor were co-deposited on Ru(0001) substrate at 10 K and annealed to 125 K with an annealing rate of 2 K min^{-1}, then waited there for 270 min.

Supporting information 3:

Table S1. Comparison of the Percentage of DME CH formation from total DME at different ratios of DME-water.

(DME:H_2O) ratio	Percentage of DME CH formation from total DME (%)
1:20	6.5
1:10	8.1
1:5	16
1:1	13

Supporting information 4:

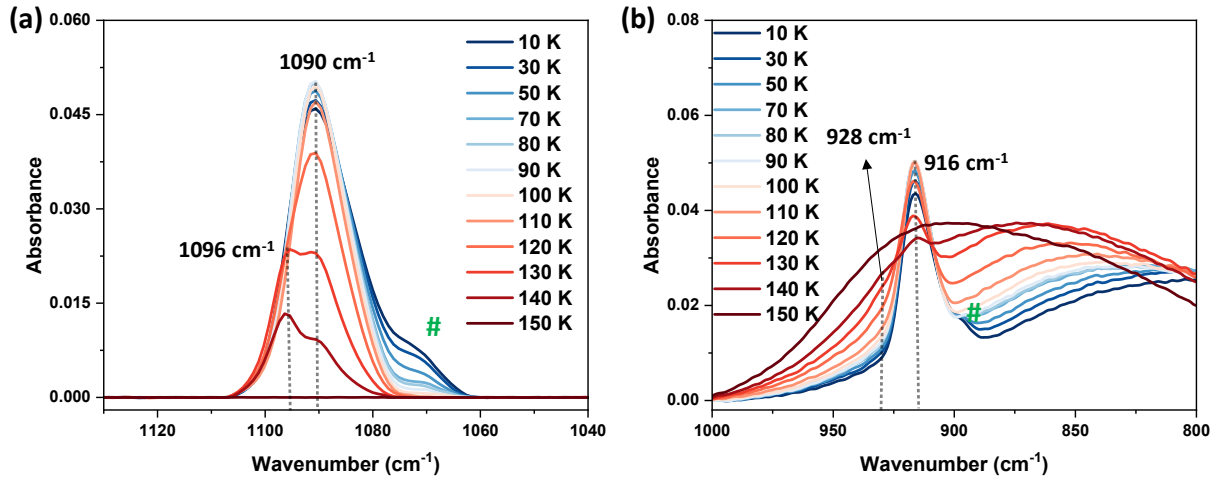

Figure S3. Temperature-dependent RAIR spectra of 300 ML of DME-H_2O (1:1) ice mixture in (a) C-O antisymmetric stretching region and (b) C-O symmetric stretching region. The peak # is attributed to the strong hydrogen bonding interaction of DME and water. DME and water vapor were co-deposited on Ru(0001) substrate at 10 K and annealed to 150 K with an annealing rate of 2 K min^{-1}.

Supporting information 5:

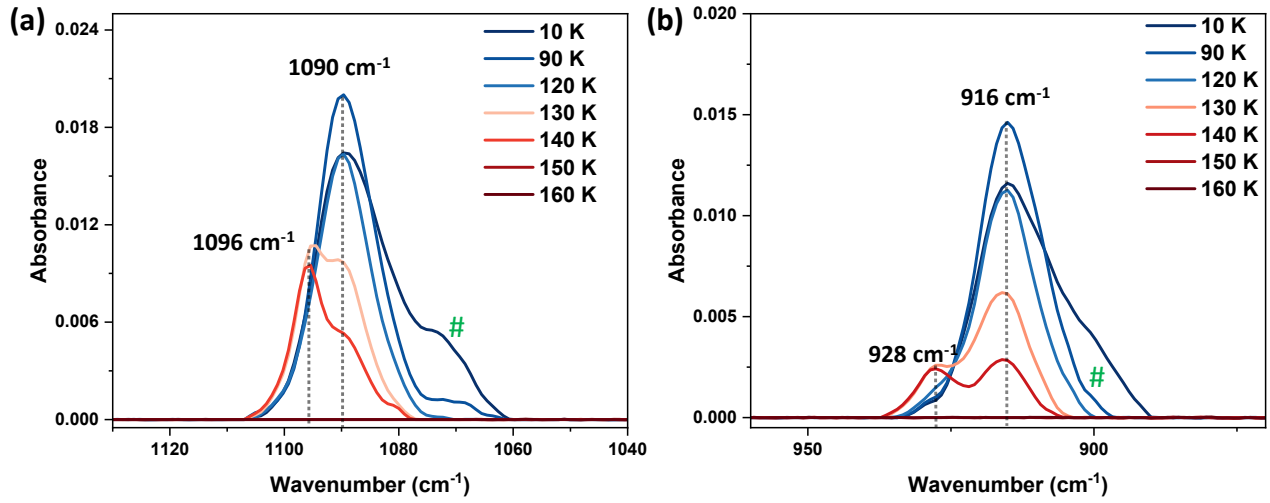

Figure S4. Temperature-dependent RAIR spectra of 300 ML of DME-D_2O (1:1) ice mixture in (a) C-O antisymmetric stretching region and (b) C-O symmetric stretching region. The peak # is attributed to the strong hydrogen bonding interaction of DME and water. DME and water vapor were co-deposited on Ru(0001) substrate at 10 K and annealed to 160 K with an annealing rate of 2 K min^{-1}.

Supporting information 6:

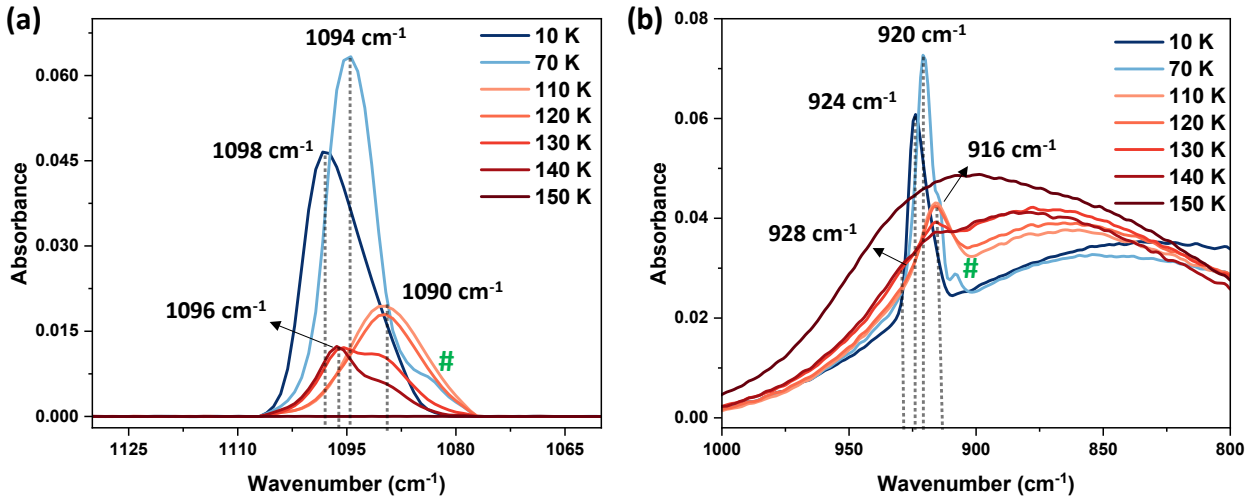

Figure S5. Temperature-dependent RAIR spectra of 300 ML of DME@H_2O (1:1) ice mixture in (a) C-O antisymmetric stretching region and (b) C-O symmetric stretching region. The peak # is attributed to the strong hydrogen bonding interaction of DME and water. DME and water were sequentially deposited on Ru(0001) substrate at 10 K and annealed to 150 K with an annealing rate of 2 K min^{-1}. The sequential deposition was carried out by condensing 150 ML of H_2O ice over the same coverage of DME ice, thus making it a (1:1) mixture.

Supporting information 7:

Table S2. Comparison of the computational and experimental vibrational shifts of DME CH compared to free DME in the C–O antisymmetric region.

	B3LYP/6-311++g(d,p) Asymmetric stretch		**Experimental**	
System	IR asymmetric stretch (cm^{-1})	Shift (cm^{-1})	IR asymmetric stretch (cm^{-1})	Shift (cm^{-1})
DME	1190.93	NA	1098	NA
DME@5^{12}	NA	NA	NA	NA
DME@$5^{12}6^2$	1193.98	3.05	NA	NA
DME@$5^{12}6^4$	1187.72	-3.21	1096	-2

Supporting information 8:

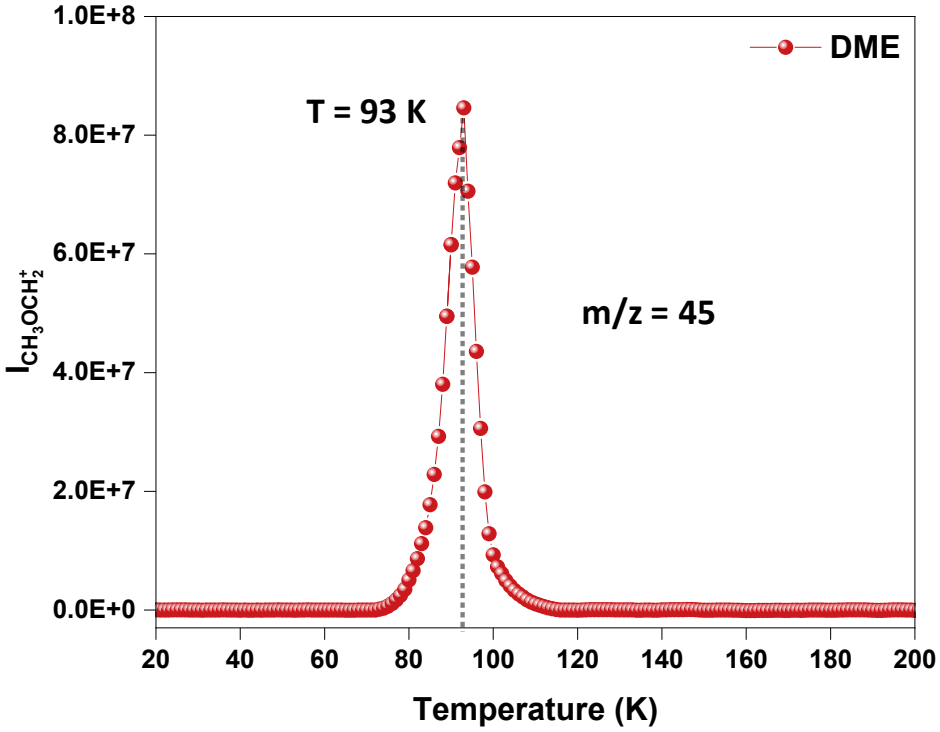

Figure S6. TPD-MS plot of 150 ML of pure DME. The intensity of $CH_3OCH_2^+$ (m/z = 45) versus the temperature of Ru(0001) substrate is plotted. The peak at 93 K is attributed to the desorption of DME. The pure DME vapor was deposited on Ru(0001) substrate at 10 K and further annealed to 200 K with an annealing rate of 10 K/min.

Supporting information 9:

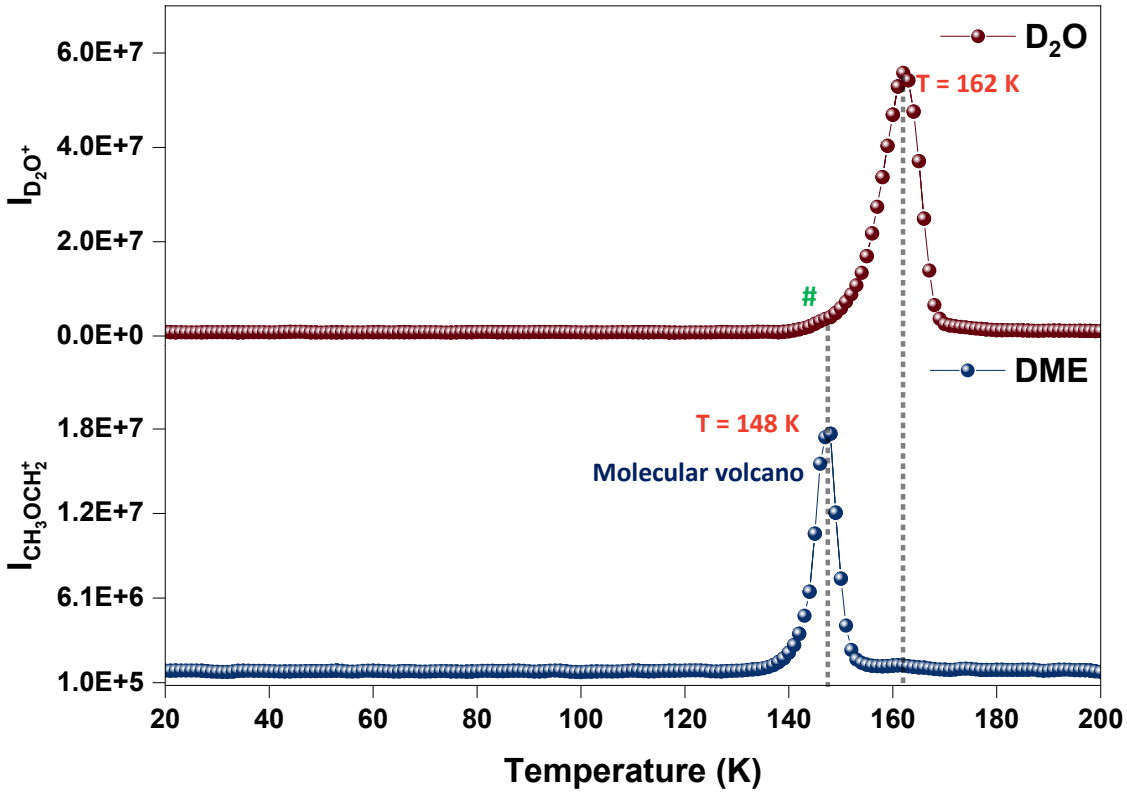

Figure S7. TPD-MS study of deuterated DME clathrate hydrate. TPD mass spectra of 300 ML of DME-D_2O (1:5) ice mixture after hydrate formation. The red spectrum represents the D_2O desorption, and the blue spectrum represents the DME desorption. Mass spectra is plotted for D_2O^+ (m/z = 18) and $CH_3OCH_2^+$ (m/z = 45) with respect to temperature. The peak labeled (#) is attributed to the phase transition from clathrate hydrate to hexagonal ice.

Supporting information 10:

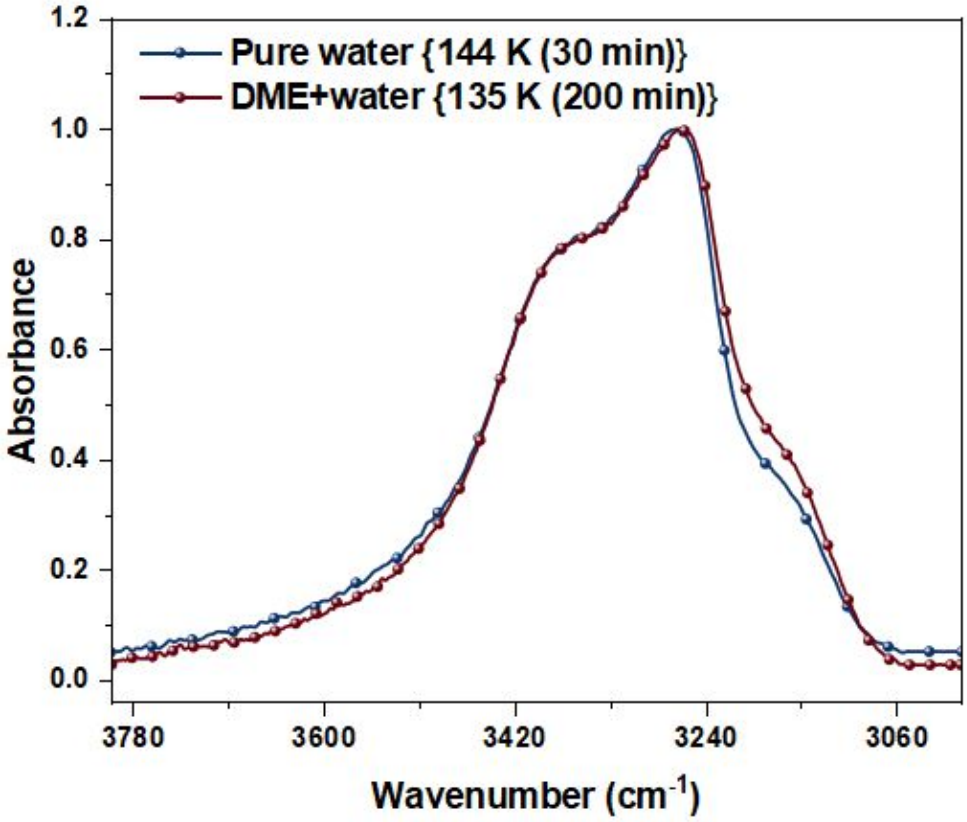

Figure S8. Comparison of the normalized RAIR spectra of hexagonal crystalline ice obtained by thermally annealing pure water at 144 K for 30 min and DME and water ice mixture (1:5) at 135 K for 200 min.

Supporting information 11:

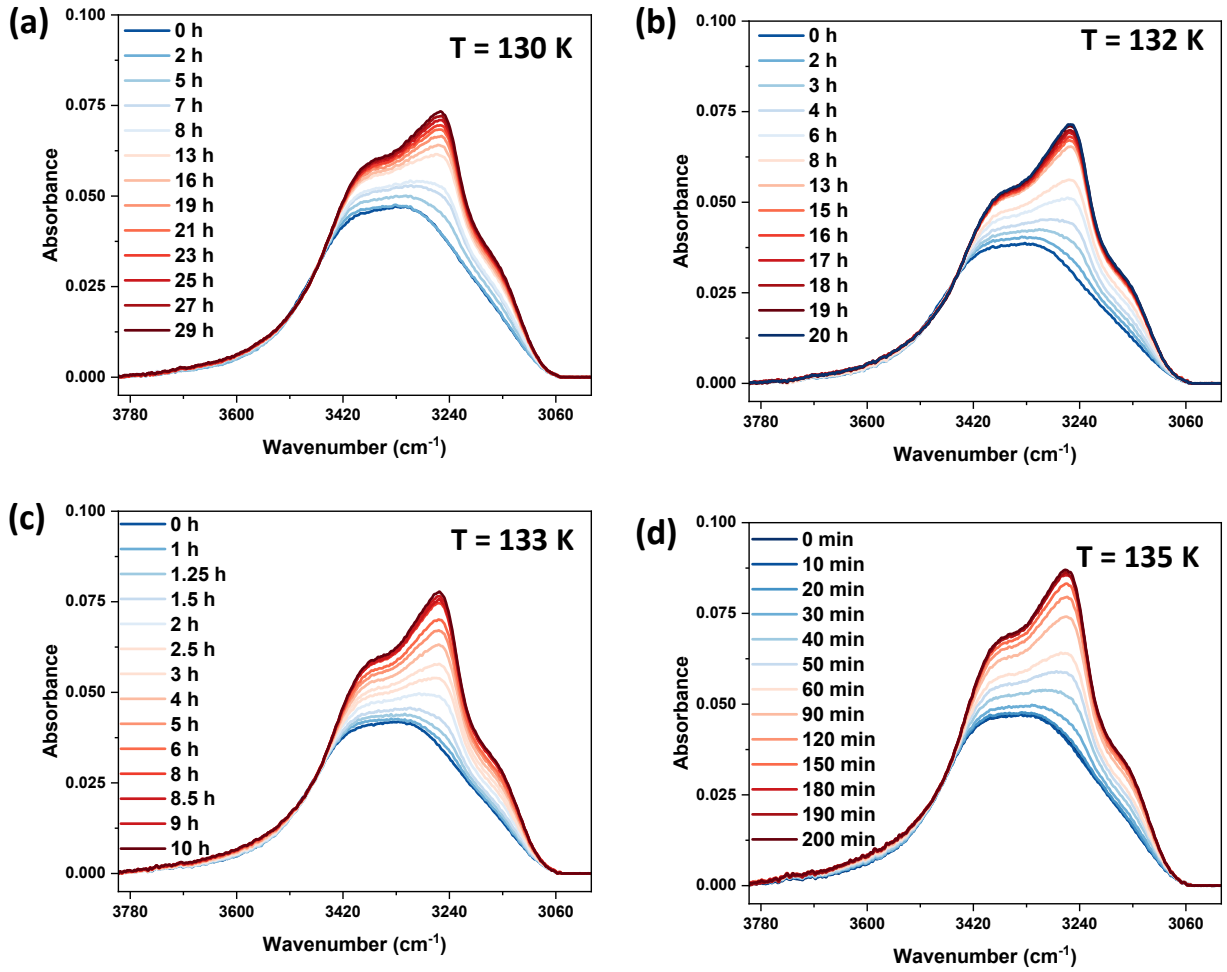

Figure S9. RAIR study of phase transition from amorphous solid water to hexagonal ice through clathrate hydrate dissociation. Isothermal time-dependent RAIR spectra of 300 ML of DME-H_2O (1:5) in the O-H stretching region at (a) 130 K, (b) 132 K, (c) 133 K, and (d) 135 K. DME and water vapor were co-deposited on Ru(0001) substrate at 10 K and annealed at a rate of 2 K min^{-1} to the set temperatures.

Supporting information 12:

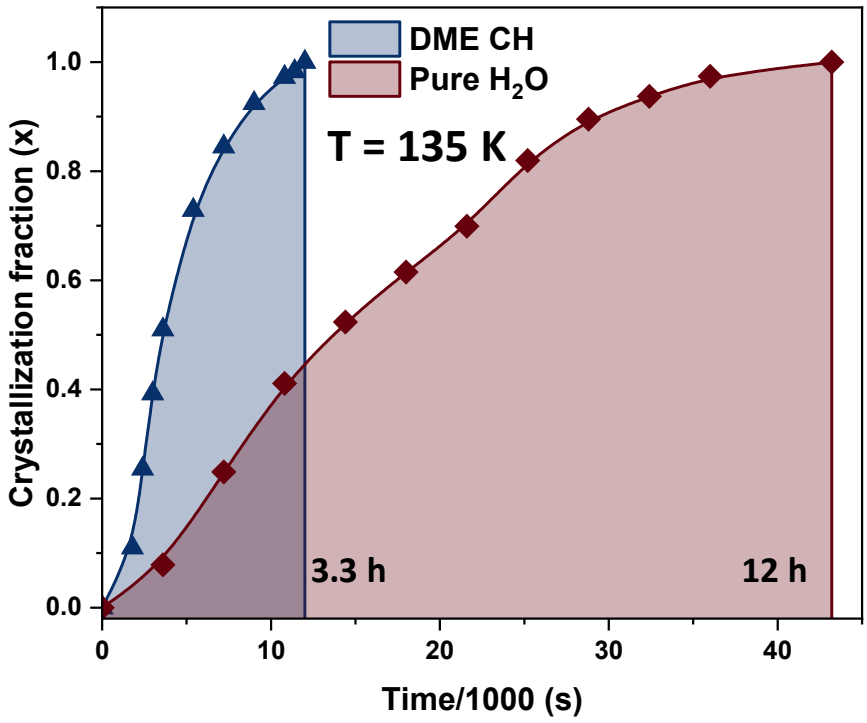

Figure S10. Crystallization fraction vs time for 300 ML of DME-H_2O (1:5) (blue color curve) and 150 ML of pure H_2O ice (brown color curve) at 135 K.